

The increase of stability of Li_xCoO_2 electrodes of cointercalated sodium

Jana Bludská, Jiří Vondrák*, Pavel Stopka and Ivo Jakubec

Institute of Inorganic Chemistry, Czechoslovak Academy of Sciences, Majakovského 24, 16000 Praha 6 (Czechoslovakia)

(Received March 23, 1990; in revised form March 26, 1992)

Abstract

Cyclic electrochemical deintercalation and intercalation of LiCoO_2 was studied in LiClO_4 /propylene carbonate electrolyte. The stability of the material was markedly improved if 10 to 20% of lithium atoms were replaced by cointercalated sodium. The increase of the stability is explained by preventing of complete deintercalation in anodic range due to essentially lower mobility of sodium ions in the van der Waals gaps.

Introduction

Mizushima *et al.* [1] proposed the use of LiCoO_2 as the positive electrode in secondary lithium batteries. Since, several papers have reported various properties of lithium and sodium intercalation compounds LiCoO_2 and NaCoO_2 as electrode materials.

The structure of these substances is a layered one [2, 3]. Generally, they are prepared by sintering of carbonates in air at 900 to 1000 °C. Although similar in structure, they differ in various properties. First, the coordination of lithium differs from that of sodium. Second, the lattice parameter c of the lithium system decreases with increasing lithium concentration [4] indicating the stabilization of the unstable CoO_2 matrix by lithium [5] and its electric field. On the contrary, expansion of c is the more usual case, although such anomalous behaviour is known as well, for example, in Li_xWO_3 system [6]. Also, the electronic properties of both species are different.

The chemical diffusion coefficient of lithium, $5 \cdot 10^{-12} \text{ m}^2/\text{s}$, is quite high if compared with other oxide materials [7]. The value of the diffusion coefficient of sodium, $D_{\text{Na}^+} = 10^{-12} \text{ m}^2/\text{s}$ was found by Stoklosa *et al.* [8].

The electrochemical intercalation/deintercalation proceeds via the reaction:



$$x + y \leq 1$$

on which the use in lithium batteries is based. Unfortunately, the delithiated CoO_2 is not stable and undergoes irreversible changes. Some of these originate in the high anodic potential at low lithium concentration (4.5 V versus Li or more); they were overcome by proper choice of aprotic solvent [9]. Nevertheless, the process of material degradation remains if the stoichiometric coefficient of lithium x is lower than 0.6 to 0.3.

*Author to whom correspondence should be addressed.

An interesting idea was introduced by Moshtev *et al.* [10, 11]. According to them, the reversibility and performance of LiCrS_2 was markedly improved if 10% of lithium was replaced by sodium. Due to the greater ionic radius of sodium, the Na^+ ions keep the van der Waals gaps more open and the mobility of lithium is increased.

The aim of the present work was to investigate the influence of a similar exchange of lithium by sodium in LiCoO_2 , with more attention being paid to the stability of the intercalated material.

Experimental

Electrode material

The cointercalation compound $\text{Li}_y\text{Na}_x\text{CoO}_2$ was prepared from a mixture of lithium, sodium, and cobalt carbonates. Commercially-available Li_2CO_3 was contaminated by sodium, and therefore, it was necessary to use pure Li_2CO_3 for the synthesis of some samples. For this purpose, lithium chloride, LiCl , was purified by crystallization from amylalcohol, in which NaCl is almost insoluble. Then, lithium carbonate, Li_2CO_3 , was prepared by precipitation of the LiCl by $(\text{NH}_4)_2\text{CO}_3$ (AR), and it was used for the preparation of pure LiCoO_2 .

The various carbonates were mixed thoroughly and calcined at 400 °C for 30 h. Pellets were made from the mixture afterwards and heated to 650 °C for 8 h. Then they were reground and new pellets were formed and heated at 950 °C for another 8 h. Their composition was checked analytically; the nominal and actual compositions of all samples are denoted as x and x' and are given in Table 1. The role of impurities and residual content of sodium in all reagents seem clear from the difference between the nominal and actual compositions.

The X-ray diffraction lines of three samples are shown in Table 2. The lattice parameters agree with published values and are not influenced by the presence of sodium.

X-ray energy-dispersive spectrometric microanalysis in a scanning electron microscope (TESLA BS 350) showed a uniform distribution of sodium in particles.

The materials were studied by electron spin resonance (ESR) spectroscopy. The spectrum of pure LiCoO_2 contained only one band, while two overlapping bands were observed on the spectra of all cointercalated substances. An example of such a spectrum is shown in Fig. 1. These spectra were treated in a conventional way. The band

TABLE 1

Nominal and actual sodium content x in $\text{Li}_{1-x}\text{Na}_x\text{CoO}_2$ samples

x (nominal)	x' (actual)
0 ^a	< 0.03
0	0.070
0.02	0.095
0.05	0.125
0.075	0.157
0.1	0.185
0.2	0.257

^aThe sample prepared from pure Li_2CO_3 .

TABLE 2

Lattice distances for three samples of $\text{Li}_{1-x}\text{Na}_x\text{CoO}_2$

Indexes <i>hkl</i>	Lattice distances d (Å)		
	$x < 0.03$	$x = 0.070$	$x = 0.095$
0 0 3	4.69	4.71	4.69
0 0 6	2.340	2.35	2.34
0 1 2	2.305	2.305	2.305
1 0 4	2.00	2.002	2.003
0 1 5	1.84	1.843	1.840
1 0 7	1.55	1.550	1.550
0 0 9	1.55	1.557	1.548
0 1 8	1.42	1.426	1.424
1 1 0	1.408	1.410	1.408
1 1 3	1.350	1.349	1.347
0 2 1	1.220	1.215	1.217

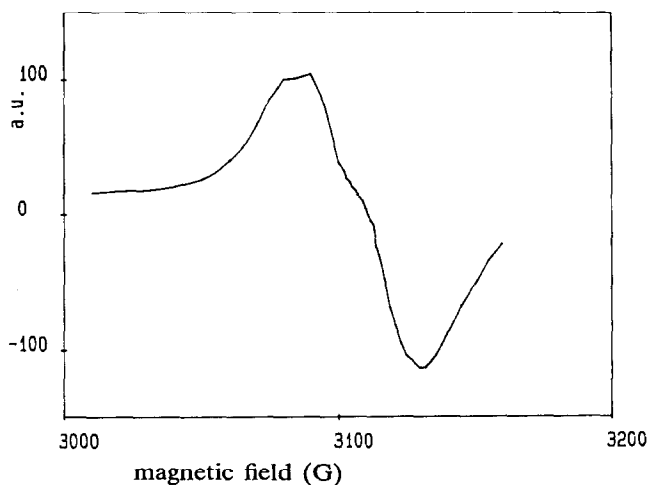


Fig. 1. The electron spin resonance spectrum of material with actual sodium concentration: $x=0.095$ (schematically, in arbitrary units).

occurring at higher magnetic field increased with increasing sodium content. A separate paper concerning this phenomenon will be published elsewhere.

Cell fabrication

The cathode material was finely ground and used as a plastic-bonded electrode. Two kinds of electrode materials were used:

- (i) pure $\text{Li}_{1-x}\text{Na}_x\text{CoO}_2$ with 10% of polytetrafluoroethylene (PTFE) powder;
- (ii) a mixture of 75% of active substance with 25% of teflonized carbon black (containing 25% of PTFE).

The composite was deposited on a platinum or stainless steel screen, wrapped in an aluminium foil, and pressed. The screen (diameter: 12 mm) was fastened onto a platinum screw (M 2, i.e., diameter 2 mm) on a PTFE holder.

A three-electrode vessel with glass-to-plastic screw joints was used, containing lithium counter and reference electrodes.

All potentials are related to a lithium reference electrode in the same solution; experiments were performed at room temperature (*c.* 20 °C). The solution of 1 M LiClO₄ in propylene carbonate (PC) was used as the electrolyte.

Methods

The aim of this work was to investigate the degradation of the electrode material at high anodic voltage. Therefore, experimental conditions were chosen so that the degradation was accelerated. Each experimental run consisted of several cycles. In each cycle, the electrode was exposed to lithiation by cathodic chronopotentiometry at a current load of 10 mA/g LiCoO₂ until the potential dropped to 1.5 V. The length of the plateau, position of the inflexion point, and the slope at the same place were evaluated from recorded *E-t* curve. Then, the electrode was polarized anodically to various potentials (4.5 V in most cases) for 1 to 5 h or overnight (*c.* 16 h), and another cycle was started. The anodic current was not recorded, as a rather high background current was included in it. The most probable origin of this was the anodic oxidation of electrolyte (PC).

A simple numeric treatment was used for the description of the chronopotentiometric curves. In general, each curve passes through a plateau with low slope and it ends at a point where the slope is the highest. For example, let us assume the validity of Crandall–Faughnan–Armand isotherm for the description of an equilibrium discharge curve:

$$E = E^0 + E^1x - RT/F \ln x/(1-x) \quad (1)$$

where E^0 is standard potential and E^1 is the Armand potential. Then, the point of lowest slope corresponds to $x=0.5$, i.e., to the concentration equal to $0.5 c_{\max}$ and the slope is given by the formula:

$$|dE/dt| = E^1 i/2Q \quad (2)$$

Here, Q is the total amount of charge obtained by the discharge of the electrode.

Therefore, the value of the lowest slope and corresponding potential were used for evaluation of the properties of all chronopotentiograms in this work, even if they are not equilibrium discharge curves.

For this purpose, the curves were differentiated numerically, and both points of minimum and maximum slopes were found, and the potential of the plateau and the total charge were evaluated.

Results

Galvanostatic charge/discharge

A typical record of potential is shown schematically (with arbitrary units on horizontal axis) in Fig. 2. Generally, the first cathodic cycle was extremely short and almost no plateau was apparent on the record, while all subsequent cycles were fairly well developed. This indicated that the lithium content in the electrode cannot exceed $x=1.0$.

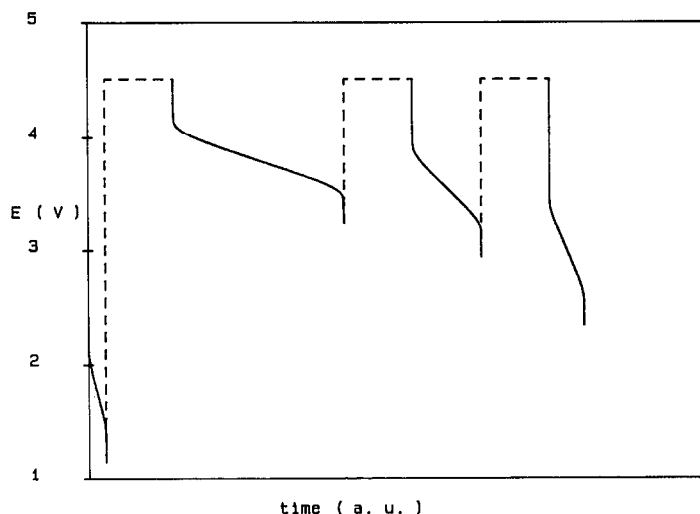


Fig. 2. The record of potential during one series of experiment (schematically, in arbitrary time units); the electrode $x' = 0$ (actual concentration).

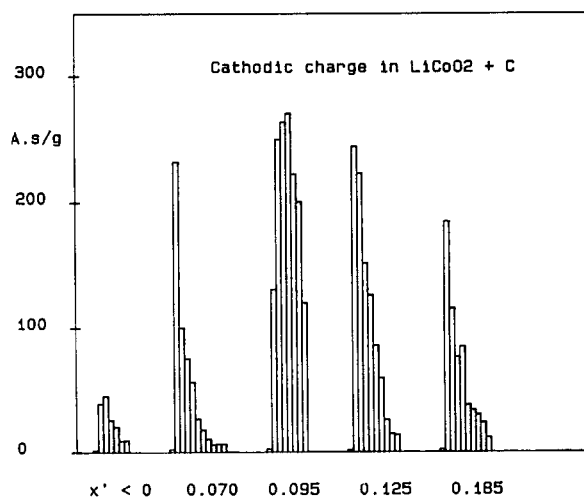


Fig. 3. The cathodic charge of electrodes containing carbon black; anodic polarization 4.5 V ($300 \text{ A s/g} = 83.3 \text{ mA h/g}$).

In Fig. 3, the cathodic charge is plotted for all materials under investigation in the form of a histogram. Similarly, Fig. 4 shows (in logarithmic scale) the slope $|dE/dt|$ at the inflex point of the plateau. In these experiments, electrode material containing carbon black and an anodic potential of 4.5 V were used.

Figure 5 describes similar experiments performed with electrode material which contained no carbon black; the potential of anodic deintercalation was 4.0 V.

Finally, the plateau potential (defined as the inflexion point) is shown in Fig. 6 (solid line for electrode with carbon black, dotted line for the other one).

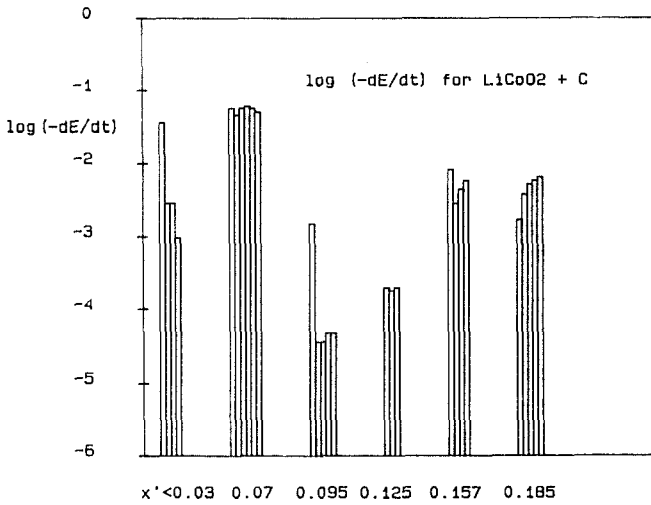


Fig. 4. The slope $|dE/dt|$ (in logarithmic scale) at inflexion points (the same electrodes).

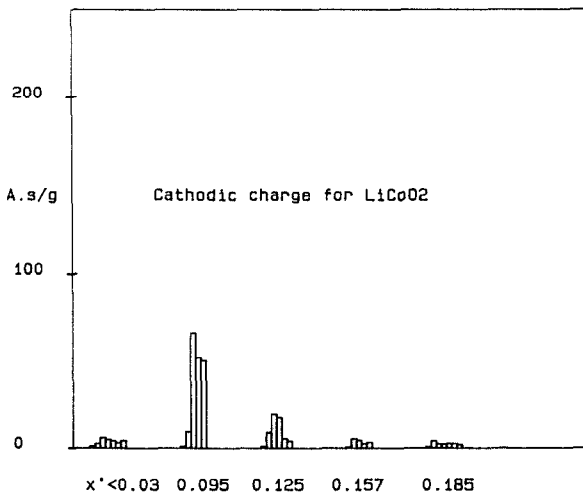


Fig. 5. The cathodic charge of electrodes without carbon black; anodic polarization: left, 3.8 V; right, 4.0 V ($300 \text{ A s/g} = 83.3 \text{ mA h/g}$).

Electrode admittance

For better explanation of electrochemical processes in cointercalated cobalt oxide, the electrochemical admittance of these materials was measured at two potentials. One potential value (2.5 V) was chosen below the intercalation range, while the other (3.9 V) is within it. Typically, a behaviour of a strongly-polarized electrode was observed at 2.5 V; the electrode admittance was rather low and its nature was that of a nonideal capacity (phase angle close to 80°). On the contrary, rather high real admittance accompanied by a diffusional Warburg component was observed at 3.9 V. The results are summarized in Table 3. Examples of the admittance spectra are shown in Figs. 7 and 8.

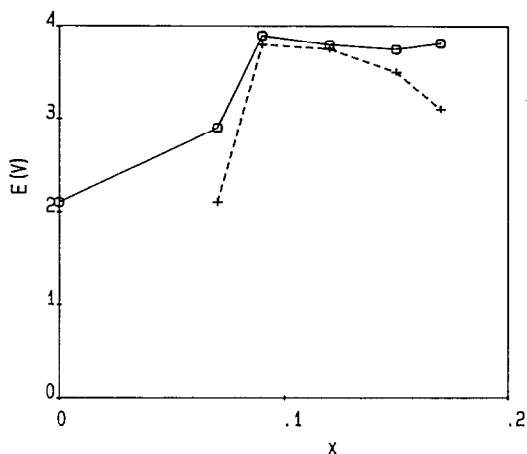


Fig. 6. The potential of inflexion points of the same electrodes; full-line electrodes with addition of carbon black, dotted-line electrodes without carbon black. Second cathodic process was considered.

TABLE 3

The components of equivalent circuits of electrode materials with actual sodium concentration x at potential 2.5 and 3.9 V; weight of sample m is in g. Conductance G_1 and G_2 are in mS, capacity C in mF, and Warburg admittance W in $\text{mS Hz}^{-1/2}$. The value $1/G_1$ is the series resistance with the parallel combination of all others

x	E (V)	m (g)	G_1 (mS)	C (mF)	W (mS Hz)	G_2 (mS)
<0.03	2.5	0.064	0.113	0.34	0.0054	0.016
	3.9		0.52			0.187
0.070	2.5	0.067	0.52	0.46	7.1	0.007
	3.9		0.75			
0.095	2.5	0.055	0.50	0.23	15.4	0.0018
	3.9		0.59			
0.125	2.5	0.044	0.83	0.34	0.15	
	3.9		0.47			0.064

Discussion

Electrode resistivity

From comparison of Figs. 2, 4, and 5 we see that the electrical conductance of the material was not sufficient to deliver a current of 10 mA/g without the addition of conductive carbon black. Moreover, essentially higher voltage was observed on materials which contained sodium. This can be explained as an improvement of electric conductivity by the presence of sodium ions in the cointercalated component. There is also a slight increase of series conductance of electrodes cointercalated with sodium, as we see from Table 3. This component of the equivalence circuit seems to increase both with sodium content and the delithiation.

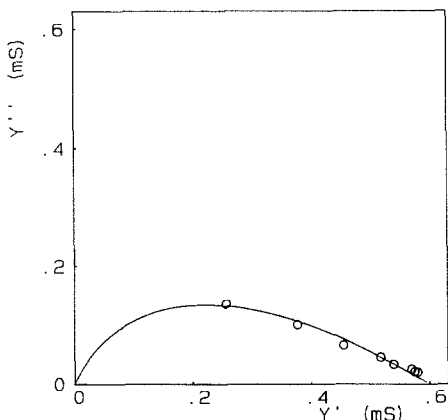


Fig. 7. The admittance of the electrode of actual composition $x=0.095$ plotted in complex plane scale at 2.5 V. The frequencies change from 0.001 Hz (left) to 10 Hz (right).

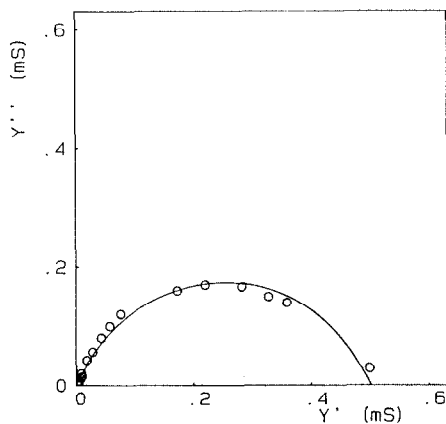


Fig. 8. The admittance of the electrode of actual composition $x=0.095$ plotted in complex plane scale at 3.9 V. The frequencies change from 0.001 Hz (left) to 0.1 Hz (right).

Electrochemical properties

The amount of electricity obtained from the electrodes is the best on materials with an intermediate degree of cointercalation. Also the slope at the inflexion point is lower (see Fig. 4) and the curves are better developed on cointercalation species.

However, the explanation of observed changes is difficult. Two factors should be considered. First, the motion of lithium in the crystals of LiCoO_2 becomes easier in the process of cyclic deintercalation/intercalation, and the slope of the discharge curves should decrease. Second, the material undergoes irreversible changes under the condition of deintercalation (i.e., at 4.5 V). If just the active surface area changes in this process, then the slope of the discharge curve should be inversely proportional to the electrode capacity, expressed as an amount of electricity, and it would change even more on real electrodes.

The data in Fig. 4 indicate that the first process is prevailing at lower concentrations of sodium, yielding in constant or even decreasing value of $|\log(dE/dt)|$. On the other hand, a marked increase of the slope observed on the two rightmost samples in Fig. 4 corresponds at least roughly to the decrease of the charge and it should be explained by the latter mechanism.

The best performance was observed for material of nominal composition $x=0.05$ (i.e., of actual sodium content $x'=0.095$). For comparison, Moshtev *et al.* [10] and Manev *et al.* [11] recommended the best content of sodium in LiCrS_2 equal to 0.1.

The values of diffusional Warburg component of the electrode admittance seem to support the first hypothesis, i.e., the promotion of lithium mobility by the presence of cointercalated sodium. Again, the value of Warburg component is the lowest if the actual lithium concentration approaches 0.1 (see Table 3).

The influence of sodium on the plateau potential (see Fig. 6) seems quite markedly expressed. Perhaps it indicates that the electrical conductivity of the material is increased by the doping the sodium, as it follows from different properties of pure LiCoO_2 and NaCoO_2 .

However, even the best samples operated with a maximum capacity of 250 A s/g (i.e., 69.4 mA h/g) of oxide and the capacity never reached the theoretical limit

974 A s/g (270 mA h/g). Apparently, few factors are responsible for that. First, the rather high cathodic current load does not allow the electrode to saturate completely with lithium. Second, the regime of discharge/charge cycles was chosen with the aim of accelerating the degradation of active material. Finally, the diffusion coefficient of sodium in the CoO_2 host lattice is significant and the sodium is removed in small amounts from the active material during consequent anodic deintercalation, together with lithium. It would be interesting to repeat these experiments with a cointercalated element other than sodium.

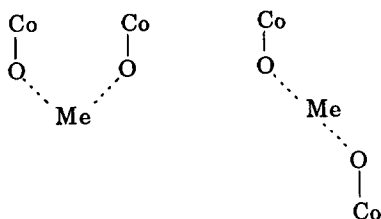
The total charge delivered by the electrode was estimated as the sum of cathodic charges of all cathodic cycles of an electrode. For the best one, it reached 1270 A s/g (352 mA h/g), which exceeds slightly the theoretical capacity of the electrode. Hence, the best material acts as a partly reversible intercalation cathode.

Electrode admittance

From Table 3 we see, that no significant difference is apparent on admittance spectra at 2.5 V. The high diffusional component, which was found at the potential within intercalation range, indicates diffusional control of the process. Moreover, we see from Table 3, that the diffusion of lithium is easier in cointercalated materials than in pure LiCoO_2 .

Structural considerations

An attempt was done to correlate the observed phenomena with the structure of the matter. The crystal structure of LiCoO_2 consist of layers containing three planes. The outer layers are occupied by oxygen and the inner ones by cobalt. Alkali metal atoms enter the interlayer gap. If we denote the alkali metal by M, then either of the following configurations is possible:



If Me is an ion of lithium, then the intensity of the electric field is undoubtedly much stronger than that in the presence of sodium ion. Therefore, greater distortion should appear and it should influence other properties of the system as its electric conductivity, ESR spectrum, mobility of lithium ion or chemical stability.

Several ideas seem to explain the observed phenomena. For example, Plichta *et al.* [12] assumed phase changes to be the interpretation of potential and overpotential changes in the discharge process in LiCoO_2 system. As the structure of NaCoO_2 undergoes a different series of phase changes [13], then the presence of sodium in the lattice should influence both the equilibrium and the kinetics of phase changes.

Another idea should be based on the electrocatalytic oxidation of PC from the electrolyte at or over 4.5 V, used in this work for accelerated degradation of the electrode material in the charging process. However, there is no experimental data available at the moment to discuss this hypothesis.

References

- 1 K. Mizushima, P. C. Jones, P. J. Wiseman and J. B. Goodenough, *Mater. Res. Bull.*, **15** (1980) 783.
- 2 H. J. Orman and P. J. Wiseman, *Acta Crystallogr. C40* (1984) 12.
- 3 J. Molenda, C. Delmas, P. Dordor and A. Stoklosa, *Solid State Ionics*, **12** (1989) 437.
- 4 A. Honders, J. M. der Kinderen, A. H. W. de Witt and G. H. J. Broers, *Solid State Ionics*, **15** (1985) 265.
- 5 B. A. Bonkamp and G. A. Wiegers, *Solid State Ionics*, **13** (1983) 1193.
- 6 M. A. Wechter, H. R. Shanks and A. F. Voigt, *Inorg. Chem.*, **7** (1968) 845.
- 7 M. G. S. R. Thomas, P. G. Bruce and J. B. Goodenough, *Solid State Ionics*, **18&19** (1986) 974.
- 8 A. Stoklosa, J. Molenda and Do Than, *Solid State Ionics*, **15** (1985) 211.
- 9 E. Plichta, M. Salomon, S. Slane and M. Uchiyama, *J. Power Sources*, **21** (1987) 25.
- 10 R. V. Moshtev, V. Manev, A. Nassalevska, G. Pistoia and M. Icovi, *J. Electrochem. Soc.*, **128** (1981) 1399.
- 11 V. Manev, R. V. Moshtev, A. Nassalevska, A. Gushev and G. Pistoia, *Solid State Ionics*, **13** (1984) 181.
- 12 E. Plichta, S. Slane, M. Uchiyama, M. Salomon, D. Chua, W. B. Ebner and H. W. Lin, *J. Electrochem. Soc.*, **136** (1989) 1865.
- 13 J. J. Braconnier, C. Delmas, C. Fouassier and P. Hagemuller, *Mater. Res. Bull.*, **15** (1980) 1797.